Cheng, Qiang; Kaario, Ossi; Ahmad, Zeeshan; Vuorinen, Ville; Larmi, Martti

Effect of pilot fuel properties on engine performance and combustion stability in a tri-fuel engine powered by premixed methane-hydrogen and diesel pilot

Published in:
International Journal of Hydrogen Energy

DOI:
10.1016/j.ijhydene.2021.09.053

Published: 29/10/2021

Document Version
Publisher's PDF, also known as Version of record

Available online at www.sciencedirect.com

ScienceDirect

journal homepage: www.elsevier.com/locate/he

Effect of pilot fuel properties on engine performance and combustion stability in a tri-fuel engine powered by premixed methane-hydrogen and diesel pilot

Qiang Cheng *, *Ossi Kaario*, *Zeeshan Ahmad*, *Ville Vuorinen*, *Martti Larmi*

Department of Mechanical Engineering, Aalto University, 02150 Espoo, Finland

HIGHLIGHTS

- Three pilot fuels are selected to investigate the effect of pilot fuel properties on tri-fuel combustion.
- Pilot fuel with high cetane number and/or low aromatic content promotes the ignition and combustion processes.
- High cetane number and/or low aromatic content of pilot fuels improve combustion stability.
- The optimized hydrogen ratio is up to 60% depends on the charge-air temperature to avoid heavy knocking.
- *Superlets* is applied to resolve high temporal-frequency resolution for combustion stability.

GRAPHICAL ABSTRACT

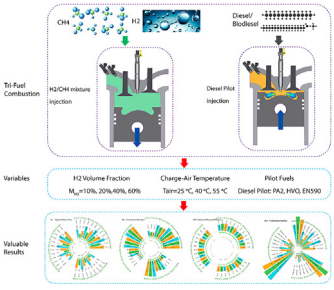

ARTICLE INFO

Article history:
Received 9 July 2021
Received in revised form
3 September 2021
Accepted 4 September 2021
Available online 24 September 2021

Keywords:
Tri-fuel combustion
Pilot fuel
Fuel properties

ABSTRACT

The present work investigates the effect of pilot fuel properties on TF combustion using premixed methane-hydrogen-air (CH_4-H_2-air) mixtures ignited by a small amount of diesel pilot. Especially, we are investigating the effect of the cetane number (CN) and aromatic content (AC) on TF combustion in a single-cylinder compression ignition (CI) engine at varying charge air temperatures (T_{air} = 25 °C, 40 °C, 55 °C) and H_2 volume fractions (M_{H2} = 10%, 20%, 40% and 60%) at lean premixed charge mixture conditions (equivalence ratio φ = 0.5). The novelty and main findings of the work consist of the following features: 1) besides the effect of H2 concentration and charge-air temperature, pilot fuel properties also play a crucial role in TF combustion, even a small amount of diesel pilot could dramatically affect the engine performance and combustion stability, 2) the CN and AC are the key factors affect the ignition delay time (IDT) and indicated thermal efficiency (ITE), 3)

* *Corresponding author.*
E-mail address: qiang.cheng@aalto.fi (Q. Cheng).

https://doi.org/10.1016/j.ijhydene.2021.09.053

Cetane number
Aromatic content

the in-cylinder pressure oscillation analysis based on a novel *Superlets (SL)* approach indicates that pilot fuel properties are important to the combustion states and combustion stability.

Nomenclature

AC	Aromatic content
aHRR	Apparent heat release rate
ATDC	After top dead center
CAD	Crank angle degree
CHR	Cumulative heat release
CI	Compression ignition
CN	Cetane number
CWT	Continuous wavelet transform
DF	Dual fuel
EHVA	Electrohydraulic valve actuator
EN590	Standard European diesel
HVO	Hydrotreated vegetable oil
IDT	Ignition delay timing
IMEP	Indicated mean effective pressure
ITE	Indicated thermal efficiency
LHV	Lower heating value
NG	Natural gas
SOC	Start of combustion
SOI	Start of injection
STFT	Short-time Fourier transform
SL	Superlets
$Q_{apparent}$	Apparent heat release
MFC	Mass flow controller
M_{H2}	Hydrogen mole fraction
PA2	Aromatic-free diesel
PSD	Power spectral density
$\dot{m}_{air}$	Air mass flow rate
$\dot{m}_{diesel}$	Diesel pilot mass flow rate
$\dot{m}_{H2}$	Hydrogen mass flow rate
$\dot{m}_{CH4}$	Methane mass flow rate
P_{ratio}	Pilot fuel ratio
TF	Tri-Fuel
T_{air}	Charge air temperature

Greek symbols

φ	Equivalence ratio
ΔP	Bandpass pressure

Introduction

Global warming and local pollution caused by the wide application of fossil fuels in internal combustion engines (ICEs) have been attracted many concerns in the industry and academia. It has been reported that every 1.5 °C rise in temperature might kill around 70% of the coral reefs and some of the insects may lose their habits [1]. These may cause significant environmental and societal problems. To mitigate these problems, many advanced combustion technologies and alternative fuels have been investigated to improve engine performance and simultaneously reduce emissions. Among all alternative fuels for ICE application, methane (CH_4) and hydrogen (H_2) are the most attractive candidates due to their excellent properties in combustion to achieve decarbonization [2,3].

The concept of implementing pure H_2 or CH_4 as the primary fuel ignited with diesel pilot as DF mode has been utilized for a relatively long time [4]. It has been reported that the application of DF combustion in compression ignition (CI) engines can promote the use of more readily available gaseous fuels or more efficient, advanced combustion modes [5–7]. However, either implementing sole H_2 or CH_4 as the primary fuel in the DF combustion has its inherent shortcoming. For the CH_4-diesel DF combustion, the main drawback is that the engine efficiency decreases compared to conventional diesel at low load or partial load. The unburned hydrocarbons (UHC) and carbon monoxide (CO) emissions are also higher in DF mode [8–10]. This reveals a non-optimum utilization of the gaseous fuel in ICEs. The main reason is that the combination of low temperature and very lean natural gas-air mixture inside the combustion chamber for low loads or partial load may lead to incomplete combustion [11,12]. In contrast, the advantages of H_2-diesel DF combustion have been widely reported to extend the lean mixture limits and simultaneously reduce the unburned CH_4 and CO [13–18]. The unique combustion properties of H_2 such as carbon-free, low minimum ignition energy (MIE), high flame speed and wide flammability range make it is an ideal candidate for its application in ICEs [14]. However, engines running solely with H_2 require expensive H_2 generation, storage, and transportation due to its low volumetric energy density and significant diffusivity in the air with the potential of accidental explosion. Moreover, the low power density and abnormal combustion such as knock [15,16], pre-ignition [17] and backfire [14,18] in pure H_2-fueled engines have currently limited its usage.

To overcome the drawbacks of the DF combustion in a heavy-duty compression ignition engine, an effective method is to mix the CH_4 and H_2 with a proper ratio and select proper pilot fuel to control the ignition and combustion phasing. In the engine context, igniting the CH_4 and H_2 mixture by a small amount of diesel pilot can be named tri-fuel (TF) combustion. TF combustion strategy has recently been explored as a promising way to use H2 and CH4 mixture to compensate for the challenges of pure CH_4 or H_2 combustion that possesses a higher combustion efficiency and combustion stability [19].

This is because H_2 is thought to be an excellent enhancement for CH_4-diesel DF combustion due to its burning characteristics, such as its wide flammability, very high flame speed, low ignition energy, and carbon-free combustion [20]. The proper H_2 substitution ratio in an H_2-CH_4 mixture may reduce the cycle-to-cycle variations and improve combustion stability [21,22]. The results from the author's previous study showed that H_2 addition enhances ignitability and combustion stability [23]. The addition of H_2 in the CH_4-air mixture reduces HC, CO, CO_2, and PM emissions almost linearly [24,25]. This can be explained by the smaller quenching distance and the higher H_2 combustion temperature, which dramatically improves the combustion efficiency. However, H_2 has a high-burning velocity which may increase the combustion temperature in the cylinder, thereby causing higher NOx emissions [26]. Moreover, when the addition of the H_2 exceeding a specific level, it could lead to abnormal combustion (e.g. knocking) subsequently damage the engine.

There have been numerous studies regarding CH_4-H_2 mixtures as primary fuel for ICEs, either experimentally [27–33] or numerically [34–41]. These studies mainly focused on the effects of primary fuel-air charge (H_2-CH_4-air) on engine performance and emissions. It has been shown that the addition of H_2 can increase combustion stability [42] and improve thermal efficiency [43]. However, few of those studies were concerned with the effects of pilot fuel properties.

It is well known that pilot fuel plays a crucial role in ignition delay time (IDT) subsequently affects the pilot and charge gas mixing, thereby determining the combustion phasing. During the ignition delay period, the pilot fuel rapidly decomposed and dehydrogenated. In general, a fuel with higher CN reduces IDT and improves the dual-fuel combustion efficiency due to the better thermophysical properties and mixture formation during the premixed combustion [44]. However, the aromatic-containing fuel is difficult to be decomposed or oxidized because of the heavy saturate hydrocarbons of aromatic components, which results in a lower decomposed rate and longer IDT [45,46]. The poor decomposition of aromatic fuels could also reduce combustion efficiency and stability [47].

According to the previous studies on DF combustion [8,46], the implementation of different pilot fuels may lead to different combustion characteristics and emissions in ICEs, which could also occur in TF combustion. S. Imran et al. [48] investigated the potential of the TF combustion with diesel and rapeseed methyl ester (RME) as pilot fuels to achieve a better trade-off between NOx and hydrocarbon emissions. They concluded that the pilot fuel properties are more crucial for the TF combustion due to the present of the H2, which may lead to a case of typical three stage ignition. L. Tarabet et al. [49] studied the TF combustion with eucalyptus biodiesel and natural gas (NG) enriched by various H2 quantities (15, 25 and 30 by v%). They found that due to the good ignition ability of the biodiesel pilot fuel in the engine as a result of the high cetane number and fuel bound oxygen, which could achieve higher engine performance and lower pollutant emissions compared to conventional diesel as pilot fuel. Mahmoud Gadalla et al. [50] numerically investigated the TF ignition using large-eddy simulation (LES) and finite-rate chemistry. They suggested that IDT is very important to avoid auto-ignition and relevant to heat release rate. Therefore, the higher CN or AC fuels could have a similar manner to avoid endgas autoignition and improve engine performance. Oliva et al. [51] has fundamentally studied the autoignition of LPG blends with diesel and HVO in a constant-volume combustion chamber. The results showed that fuel with higher CN such as HVO has a better autoignition behavior than biodiesel and conventional diesel. The above literature review highlights the importance of pilot fuel properties in DF and TF combustion. However, to the best of the authors' knowledge, estimating the effect of pilot fuel properties on tri-fuel engine powered by premixed methane-hydrogen and diesel pilot is yet to be comprehensively investigated.

Considering the literature review above, it is observed that CH_4 and H_2 both fuels have been extensively studied in the last decades. While, numerous studies on 1) the CH_4 or H_2 as primary fuel in DF combustion, 2) the pilot fuel properties on the CH_4-diesel DF combustion. The numerical or experimental investigation on TF combustion in a wide range of charge-air temperature and H2 concentration is still scarce. Especially, comprehensively estimating the effect of pilot fuel properties on engine performance and combustion stability is yet to be reported. Moreover, offering high-resolution in time and frequency to resolve localized intermittent periodicities of the combustion stability in the engine is equally important. However, the conventional continuous wavelet transform (CWT) or short-time Fourier transform (STFT) methods can not reveal transient oscillation events that are hidden in the averaged time-frequency spectrum. A novel spectral estimator is fairly needed to analyze the combustion stability based on the in-cylinder pressure.

With above motivation, this study provides a systematic framework to fill the gaps in the literature on TF combustion in a single cylinder CI engine fueled with different pilot fuels. The particular objectives are stated as follows:

1. Comprehensively investigate the effect of pilot fuel properties, i.e., cetane number and aromatic content on TF combustion at a wide range of H2 concentrations (e.g., $M_{H2} = 10\%, 20\%, 40\%, 60\%$) and charge air temperature (e.g., $T_{air} = 25\ ^{\circ}C, 40\ ^{\circ}C, 55\ ^{\circ}C$).
2. Clarify the effect of pilot fuel properties on the engine performance, such as ignition delay time, combustion duration, indicated thermal efficiency and combustion stability at different combustion states, i.e., normal combustion, PREMIER (PREmixed Mixture Ignition in the End-gas Region) combustion and knocking.
3. Implement a novel approach, namely, *Superlets* instead of short-time, the conventional continuous wavelet transform (CWT) or short-time Fourier transform (STFT) methods to estimate the combustion stability based on in-cylinder pressure oscillation analysis.

Experimental setup and operating conditions

Engine and measurement device specifications

Fig. 1 demonstrates the schematic of the operated engine. An AGCO 84AWI 6-cylinder common rail diesel engine is modified

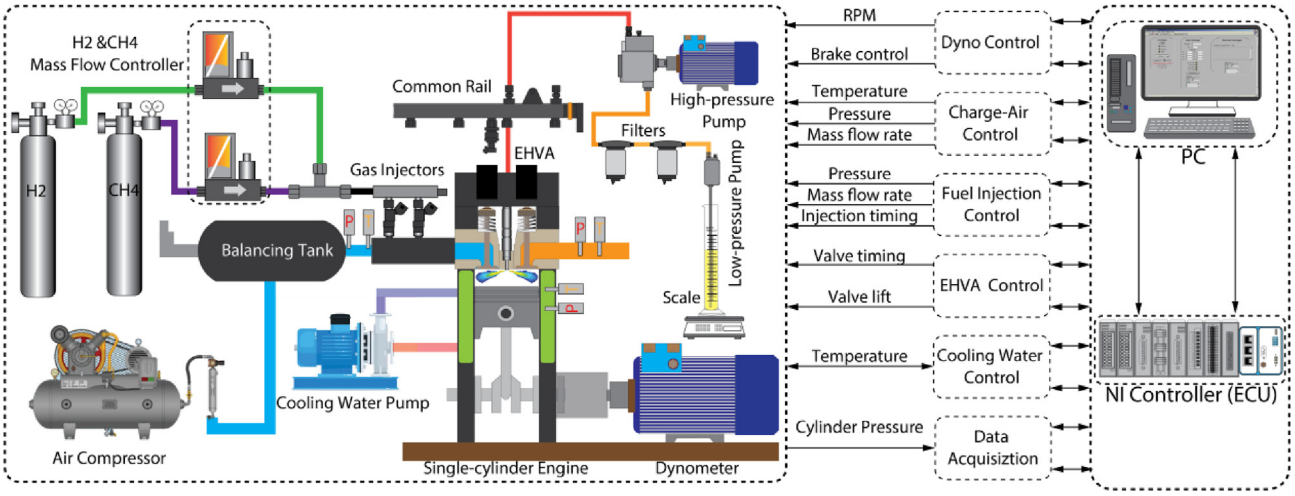

Fig. 1 – Visualization of the test engine.

to a single-cylinder engine under multiple-fuel modes (e.g., DF or TF). The engine load and speed are controlled by a 45 kW ABB low voltage motor coupled with a frequency converter (ACS800-11). An RHM-08 Coriolis mass flow meter (Rheonik Messtechnik GmbH) is adopted to measure charge-air mass flow ($\dot{m}_{air}$) and two mass flow meters/controllers (EL-FLOW®) are employed to measure port-injected CH_4 and H_2 mass flow rates ($\dot{m}_{CH4}$ and $\dot{m}_{H2}$), respectively. In this study, a closed-loop PID controller is applied to maintain the charge-air mass flow rate of 80 kg/h as the increase of charge-air temperature. The diesel pilot is provided by a Bosch CRI3 piezo injector (3-hole), which has very high stability and low delay. The well-defined CH_4-H_2 mixtures are injected by two Bosch natural gas injectors (NGI2) into the intake manifold. A crank-angle encoder is employed to acquire the crank angle signal at a revolution of 0.2°CA. A piezoelectric sensor (type 6125C, Kistler Co., Inc.) with a charge amplifier (type 5011B, Kistler Co., Inc.) at a resolution of 0.2 CAD is implemented to measure the in-cylinder pressure. Prior to the experiment, the necessary parallel systems, such as electro-hydraulic valve actuation (EHVA), charge-air conditioning, cooling, and fuel injection systems are monitored and can be flexibly controlled to achieve engine operating parameters based on the National Instrument field-programmable gate-array (NI-FPGA) and LabView software. The detailed single-cylinder engine specifications are shown in Table 1.

The most important devices to control and monitor the operating conditions are listed in Table 2, including measured variables, range and accuracy. All the devices have been calibrated or validated before the experiments based on the error analysis.

Engine operating conditions and test matrix

Table 3 shows the engine operating conditions. In this study, the engine speed, charge air mass flow, SOI, equivalence ratio, pilot duration, cooling temperature are fixed and pilot fuel, charge air temperature and the mass flow of H2 and CH4 are varied to concentrate the effect of pilot fuel properties on the TF combustion at different conditions. The engine is operated

Table 1 – Single cylinder CI engine specification.

Parameter	Value
Model	Modified AGCO 84AWI 6-cylinder CI engine
Power	200–298 kW @2100 rpm
Operating speed	1200 rpm
Bore × stroke	111 mm × 145 mm
Length of connecting rod	132 mm
Displacement volume	1402 cm^3
Combustion bowl	89.9 cm^3
Geometric compression ratio	16.7:1
Swirl Ratio	2.7
Diesel injector	Bosch Piezo CRI3 injector
Diesel injector no. of holes x diameter	3 × 0.160 mm (symmetric)
Diesel injection pressure	1000 bar
Gaseous fuel system	2 × Bosch NGI injectors
Valve System	Electrohydraulic Valve Actuator
Intake valve opening	2 CAD BTDC
Intake valve closing	210 CAD ATDC
Exhaust valve opening	225 CAD BTDC
Exhaust valve closing	6 CAD BTDC

at a lean premixed charge mixture ($\varphi = 0.5$) conditions with a constant charge-air mass flow of 80 kg/h, which provides total energy of ~130 MJ/h at 1200 rpm with a load of ~70% corresponding to the IMEP = ~13 bar. The energy share ratio of pilot fuel is 10% with an injection pressure of 1000 bar. A total of 200 continuous cycles after engine stabilization for each test point are recorded for data analysis. More details can be seen in Table 3. The experimental matrix is outlined in Fig. 2. It should be noted that the appearance of heavy knocking restricts the operation under higher M_{H2} or T_{air}.

The overarching objective of this investigation is to assess the effects of the pilot fuel properties, in particular, the CN and AC of pilot fuels on TF combustion at various H_2 fractions (M_{H2}) and charge air temperature (T_{air}) conditions. Therefore, two cases are cataloged to compare the effect of CN (Case A) and AC (Case B) on TF combustion as shown in Table 4.

Table 2 – Specification of the most important measurement devices.

Variable	Device type/model and manufacture	Range	Accuracy
Load and speed	45 KW 94 AMP MOTOR with ACS800-11 frequency converter, ABB	0–2960 rpm	±10 rpm
Valve timing and lift	EHVA, Park	0–12 mm	±0.05 mm
Cooling temperature	Cooling system, customized	0–100 °C	±1 °C
Charge-air supporter	E-turbo, customized	1–3 bar	±0.5%
Charge-air mass flow	RHM-08 Coriolis, Rheonik Messtechnik	0–200 kg/h	±0.5%
Charge-air temperature	PT100, TC	0–200 °C	±0.1%
Charge-air pressure	Piezoelectric/AVL LPD11DA05	0–5 bar	±0.1%
Cylinder pressure	6125C sensor and 5011B amplifier, Kistler	0–300 bar	≤±0.4%
Exhaust Temperature	Type K, TC	0–1000 °C	±0.5%
Exhaust Pressure	Piezoelectric/AVL GU21C	0–10 bar	±0.1%
H2 mass flow	MVM-030-PA, EL-FLOW®	1–30 L/min	±0.3%
CH4 mass flow	MVM-060-PA, EL-FLOW®	1–60 L/min	±0.3%

Table 3 – Engine operating conditions.

Parameter	Unit	Value			
Pilot fuel		PA2, HVO, EN590			
SOI	CAD BTDC	7			
$\dot{m}_{air}$	kg/h	80			
Equivalence ratio		0.5			
Pilot ratio	%	10			
Cooling temperature	°C	70			
Pilot Energy,	MJ/h	13.26			
$\dot{m}_{pilot}$	g/h	318.4			
Pilot duration	ms	0.256			
Charge-air temperature	°C	25, 40, 55			
H2 fraction	vol%	10	20	40	60
$\dot{m}_{H2}$	g/h	31.52	68.58	166.48	317.61
$\dot{m}_{CH4}$	g/h	2257	2183	1987	1685
CH4 energy	MJ/h	112.9	109.2	99.35	84.2
H2 energy	MJ/h	3.78	8.23	19.98	38.11
Total energy	MJ/h	129.7	130.4	132.6	135.9

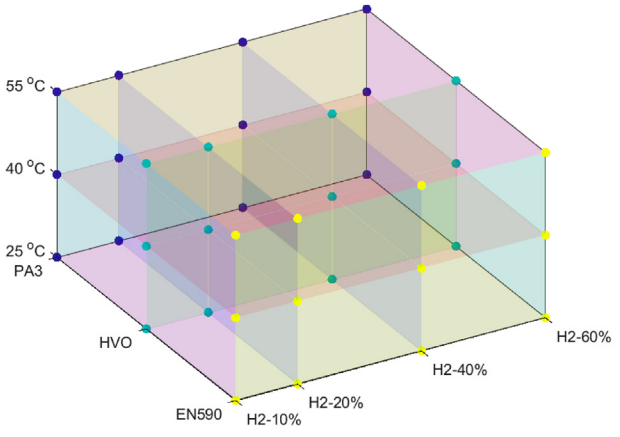

Fig. 2 – Experimental matrix.

Fuel properties

Compared to the other gaseous or liquid fuels, such as gasoline, ammonia, ethanol, methanol, dimethyl ether, etc. The advantages of implementing H_2 and CH_4 mixture as the primary fuel in TF combustion relies to 1) both CH4 and H2 are renewable and have been extensively applied as energy sources, 2) very low carbon ratio, which can reduce the CO_2 emission, 3) the complementarity of the CH_4 and H_2 in combustion characteristics can improve the combustion efficiency and simultaneously reduce the emissions, 4) both CH_4 and H_2 are gas phase, which is easy to mix.

Table 4 – Cases study of the effect of typical pilot fuel properties on TF combustion (more details are shown in Table 5).

Case Name	CN	AC, %
Case A: Effect of CN		
PA2	56	<0.1
HVO	80–99	<1.0
Case B: Effect of AC		
PA2	56	<0.1
EN590	52.6	≈30

Three pilot fuels are compared to assess the effect of pilot fuel properties, especially the CN and AC on the TF combustion. Table 5 shows the detailed properties of the pilot fuels (PA2, HVO, and EN590) and gaseous fuels. For the pilot fuels, 1) PA2 is a customized diesel-like low aromatic fuel that has a similar CN and LHV with NE590 but very low AC, 2) HVO consists of straight-chain and branched paraffin, free-of-aromatics, is a renewable diesel produced by Neste, which has high CN [49], and 3) standard European diesel EN590, which has averaged CN but relatively high AC. The high purity CH_4 and H_2 are provided by AGA Industrial Gases (Finland) with a purity of 99.95% and 99.9%, respectively.

Operating parameter and data analysis

Basic definition and methodology

(1) Definition of IDT

In the present study, the IDT is defined as the time interval between the start of pilot injection and the start of combustion.

$$IDT = \theta_{SOC} - \theta_{SOI} \quad (1)$$

where, θ_{SOC} is the start of combustion timing, which is defined as cylinder pressure rise rate (PRR) timing. θ_{SOI} is the start of

Table 5 – Physical and chemical properties of the pilot and gaseous fuels [50,52,53].

Items	Unit	EN590	PA2	HVO	Hydrogen	Methane
Molecular formula		C_{12}-C_{22}	$C_9 - C_{21}$	C_{15}-C_{18}	H_2	CH_4
Cetane Number		52.6	56	80–99	–	0
Lower heating value	MJ/kg	≈42.7	42.3	44	120	50
Total aromatics		≈30	<0.1	<1.0	–	–
Polyaromatics (PAH)		≈4	–	<0.1	–	–
Stoichiometric air-fuel ratio		14.5	14.4	15.12	34.48	17.19
Density at 15 °C, 1 atm	kg/m^3	820–845	810.2	775–785	0.09	0.725
Dynamic viscosity @ 40 °C	[mPa.s]	1.352	2.16	≤5	0.00915	0.01177
Kinematic viscosity @ 40 °C	mm^2/s	2.0–4.5	2.66	2.0–4.0	–	19.47e-6
Carbon content	wt. - %	86.5	84.94	87.2	0	20
Hydrogen content	wt. - %	13.5	14.06	12	100	80
C/H ratio	–	6.4	6.04	7.26	–	4
Autoignition Temperature	°C	250–350	250–350	204	650	585
Minimum ignition energy	mJ	–	–	–	0.02	0.3
Flammability limits	%	0.6–5.5	–	–	4–75	5–15
Burning velocity in NTP	cm/s	37–43	–	–	265–325	37–45
Quenching gap in NTP Air	cm	–	–	–	0.064	0.203
Diffusivity in air	cm^2/s	~0.07	~0.07	~0.07	0.63	0.16
Research octane number		30	–	–	130	>122
Specific heat *Cp*@300 K	kJ/kg.K	2.05	–	–	14.89 (gas)	2.22

injection timing. It should be noted that the definition of IDT is different from the IDT in conventional diesel engines, which is defined as the crank angle at 5% or 2% of cumulative heat release (CA5 and CA2) is commonly defined as IDT [54,55]. More explanation can be seen in Ref. [23].

(2) aHRR calculation

A single-zone heat release model based on the first law of thermodynamics is applied to calculate the aHRR, which is expressed as:

$$\frac{dQ}{d\theta} = \frac{\gamma}{\gamma - 1} \cdot P \cdot \frac{dV}{d\theta} + \frac{1}{\gamma} \cdot V \cdot \frac{dP}{d\theta} \tag{2}$$

where Q is the heat release, γ is the specific heat capacity ratio ($\gamma = 1.35$), θ is the crank angle, P is the cylinder pressure, V is the swept volume.

(3) IMEP and ITE

The IMEP is applied to analyze the energy conversion in TF combustion. The IMEP is derived from the following equation:

$$IMEP = \frac{1}{V_d} \int_0^{720} PdV \tag{3}$$

where, V_d is the displacement volume.

The ITE is used to evaluate the fuel energy conversion efficiency. The average value of the indicated thermal efficiency of the test engine as follows,

$$ITE = \frac{IMEP \cdot V_d}{m_{pilot} \cdot LHV_{pilot} + m_{H2} \cdot LHV_{H2} + m_{CH4} \cdot LHV_{CH4}} \tag{4}$$

where, m_{pilot}, m_{H2}, m_{CH4} are the mass of diesel pilot, H2 and CH4 per cycle. LHV_{pilot}, LHV_{H2}, LHV_{CH4} denotes the lower heating values of diesel pilot, H2 and CH4, respectively.

(4) Pilot fuel ratio (R_{pilot}) and H2 concentration (M_{H2})

The pilot fuel ratio is defined as the energy share ratio of the pilot fuel, which is expressed as:

$$R_{Pilot} = \frac{m_{pilot} \cdot LHV_{pilot}}{m_{pilot} \cdot LHV_{pilot} + m_{H2} \cdot LHV_{H2} + m_{CH4} \cdot LHV_{CH4}} \tag{5}$$

The H_2 concentration is defined as the volume fraction of the H_2 in the H_2-CH_4 mixture. In this study, the H_2 and CH_4 are controlled by two mass flow controller, thus the volume fraction of H_2 (M_{H2})is calculated based on the mass flow rate as follow,

$$M_{H2} = \frac{\dot{m}_{H2} \cdot W_{CH4}}{\dot{m}_{CH4} \cdot W_{H2} + \dot{m}_{H2} \cdot W_{CH4}} \tag{6}$$

where, $\dot{m}_{H2}$ and $\dot{m}_{CH4}$ are the mass flow rate of H_2 and CH_4, and W_{H2} and W_{CH4} are the molecular weight of the H_2 and CH_4, respectively.

Definition of TF combustion process

To clarify the combustion process, the whole combustion process is divided into IDT (PRR-based), premixed combustion (IDT→CA5) and main combustion (CA5→CA90) based on the percentage of cumulative heat release as shown in Fig. 3. Owing to the appearance of abnormal combustion at high H2 fraction or/and high charge-air temperature, the combustion states are catalogized to normal combustion, premixed mixture ignition in the end-gas region (PREMIER)combustion and knocking based on the HRR. In normal combustion, HRR shows a normal decrease after main combustion (CA50). In PREMIER combustion, there is a small HRR rebounding after CA50 due to the end-gas autoignition. However, in the knocking, an extremely strong HRR rebounding can be observed during the main combustion due to the spontaneous main combustion and end-gas burning [56,57].

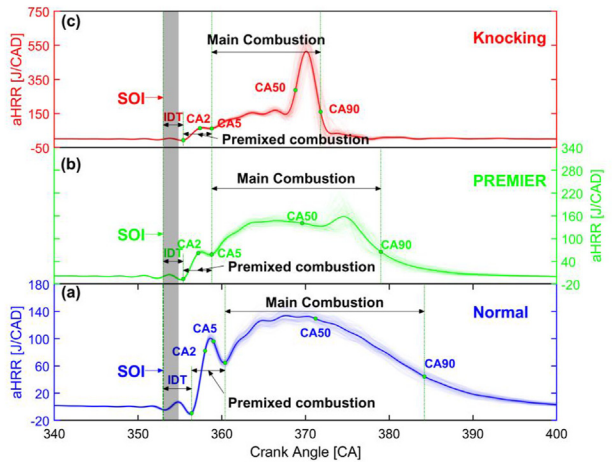

Fig. 3 – Representative pressure traces and calculated dP/dθ, HRR and CHR, and comparison of IDTs based on different definitions.

Combustion stability

To assess the effect of pilot fuel properties on combustion stability, a novel wavelet transform method, namely *superlets* (SL), is implemented to assess the combustion stability based on the in-cylinder pressure. *SL* is from optical super-resolution, which can provide a new spectral estimator to reveal transient oscillation events that are hidden in the averaged time-frequency spectrum by conventional continuous wavelet transform (CWT) or short-time Fourier transform (STFT) methods [58]. *SL* can construct a time-frequency representation of a time series that offers high-resolution in time and frequency localization, so it can resolve localized intermittent periodicities of the combustion stability in the engine. According to the SL definition, a set of Morlet wavelets with a fixed center frequency, *f*, and spanning a range of different cycles (bandwidths) will be combined to reserve the oscillation of in-cylinder pressure.

$$SL_{f,o} = \{\psi_{f,c} | c = c_1, c_2 \cdots, c_o\} \tag{7}$$

where, *o* is the order of the SL (the number of wavelets in the set), and $c_1, c_2 \cdots, c_o$ are the number of cycles for each wavelet in the set. When $o = 1$, the SL is a single (base) wavelet with c_1 cycles (can be considered as a CWT). In other words, SL is a finite set of wavelets spanning multiple bandwidths, *o* at the same center frequency, *f*. The wavelets in SL can be considered multiplicatively or additively based on the number of cycles. In a multiplicative SL, $c_i = i \cdot c_1$, whereas in an additive

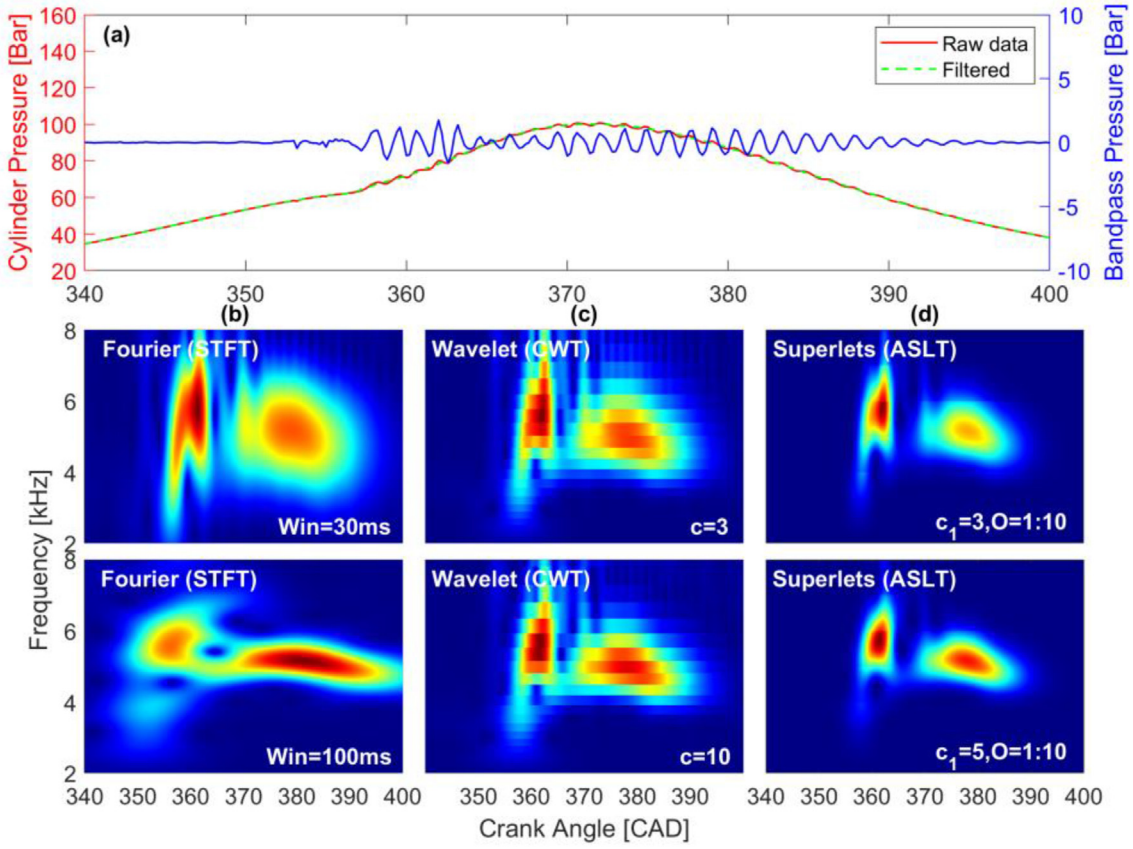

Fig. 4 – Time-frequency evaluation of cylinder pressure fluctuation with various transform approaches, (a) in-cylinder pressure, raw data, filtered and their subtraction (bandpass pressure). (b) STFT (Blackman window) with a window size of 30 and 100 ms. (c) CWT by using Morlet wavelets with the number cycle of $c = 3$ and $c = 10$, roughly matching the STFT with a window size of 30 and 100 ms. (d) Adaptive SL transform (ASLT) with linearly varying number of base cycles ($c_1 = 3$ *and* $c_1 = 5$) with order $o = 1$, for 10 Hz.

$SL\ c_i = c_1 + i - 1$, for $i = 2,\cdots,o$. Here, the response of an SL to a signal, x, can be defined as the geometric mean of the responses of individual wavelets in the set as follow:

$$R[SL_{f,o}] = \sqrt[o]{\prod_{i=1}^{o} R[\psi_{f,c_i}]} \tag{8}$$

where, $R[\psi_{f,c_i}]$ is the response of wavelet i to the signal, for instance, the magnitude of the complex convolution (for complex wavelets, such as Morlet) can be expressed as:

$$R[\psi_{f,c_i}] = |\psi_{f,c_i} * x| \tag{9}$$

where, * is the convolution operator. The SL is an estimator of the magnitude presenting the oscillation packets at the central frequency, f in the signal.

To estimate pressure oscillation intensity, the response of the SL is simply squared. As shown in Fig. 4, the SL exhibits the highest resolution compared to STFT and CWT methods when doing the cylinder pressure analysis. It shows that with

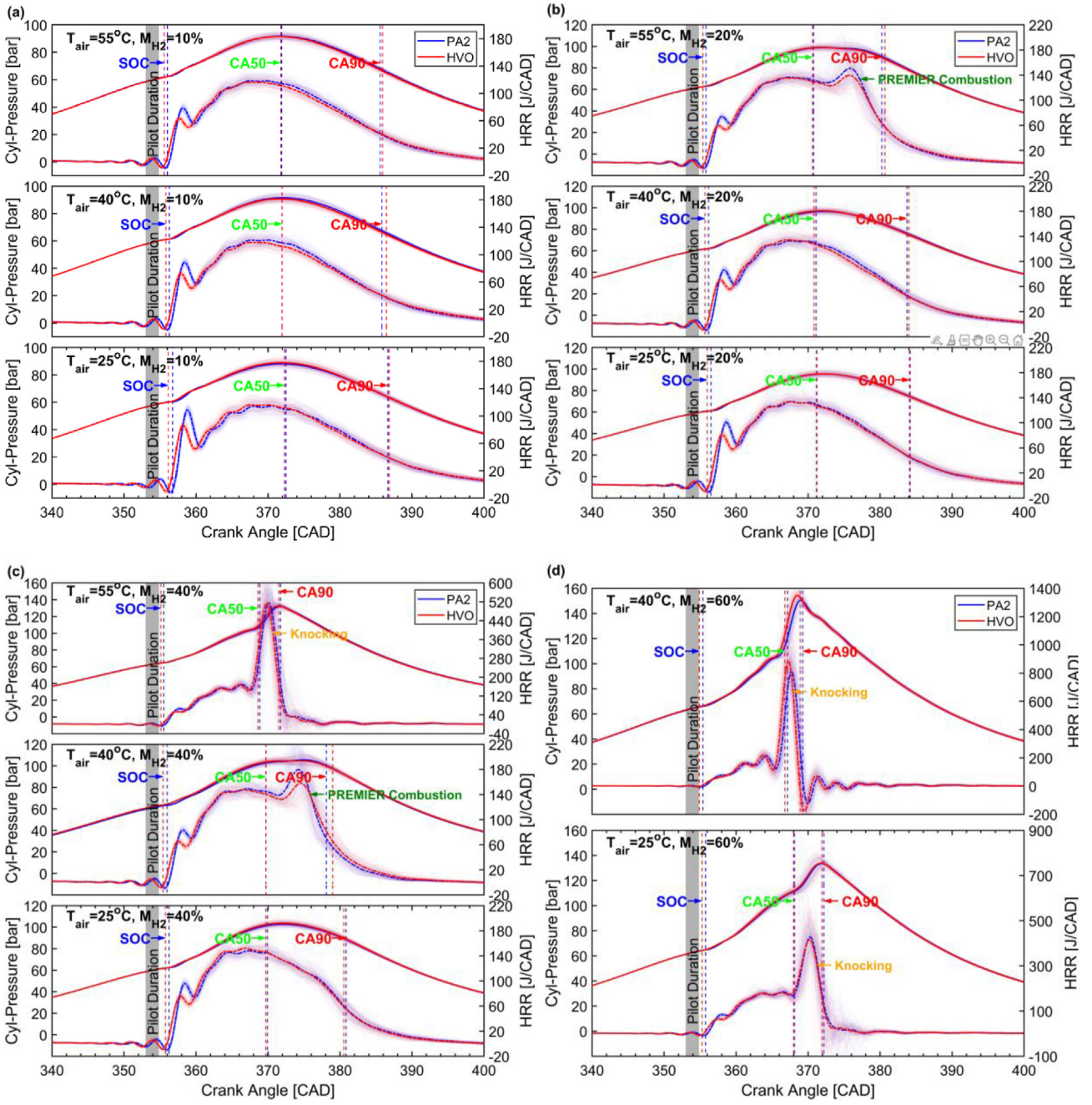

Fig. 5 – Effect of CN on in-cylinder pressure and aHRR at different M_{H2} and T_{air} conditions, (a) M_{H2} = 10%, (b) M_{H2} = 20%, (c) M_{H2} = 40%, (d) M_{H2} = 60%.

increasing frequency resolution locally, the SL does not significantly lose time resolution.

Results and discussion

Effect of cetane number (CN) on engine performance

In this section, a comprehensive comparison of the effect of CN on engine performance is investigated by comparing PA2 and HVO at a wide range of M_{H2} and T_{air} conditions.

It is well known that CN is an important ignition indicator to characterize the ignition quality of the diesel fuels in CI engines [59–61]. Fuels with a high CN can shorten the IDT, which leads to a premixing time for diesel pilot and charge mixture. Therefore, the CN of diesel pilot is a fundamental parameter to effectively control the combustion process, allowing for high thermal efficiency. Fig. 5 illustrates the effect of CN on cylinder pressure and HRR at corresponding conditions.

At low T_{air} and M_{H2} conditions (T_{air} < 55 °C and/or M_{H2}<40%), the normal combustion without pressure rebounding after CA50 can be observed in Fig. 5 (a) and (b). PA2 and HVO have a similar combustion behavior after CA50 due to the depleting of the pilot fuel. With the increase of the T_{air} or M_{H2} ($T_{air} \geq 40$ °C and/or $M_{H2} \geq 20\%$), the PREMIER combustion caused by the end-gas autoignition creates a small pressure rebounding after CA50, which is evidently presented in aHRR, as shown in Fig. 5 (b) ($T_{air} = 55$ °C and $M_{H2} = 20\%$) and Fig. 5 (c) ($T_{air} = 40$ °C and $M_{H2} = 40\%$). Owing to the effect of CN on the ignition timing, the PA2 shows an earlier end-gas autoignition timing and a higher rebounding peak in aHRR. The explanation is that the longer IDT of the PA2 leads to a more charge mixture in the end-gas region followed by stronger end-gas combustion. Further increasing the T_{air} or M_{H2} ($T_{air} \geq 55$ °C and/or $M_{H2} \geq 40\%$) as shown in Fig. 5 (c) ($T_{air} = 55$ °C and $M_{H2} = 40\%$) and Fig. 5 (d), the IDT and end-gas autoignition timing are further advanced, the violate combustion caused by the more reactive end-gas combustion leads to knocking. This is relative to the high temperature and more reactive mixtures in the cylinder, which dramatically promotes the burning rate in the main combustion and end-gas combustion region subsequent to a strong pressure oscillation. It is shown that the end-gas autoignition timing of higher CN fuel HVO is slightly earlier than lower CN fuel PA2, but a comparable knocking intensity (HRR peak) can be observed in both fuels. The interpretation is that the IDT is very short and the burning rate of the charge mixture in the main and end-gas combustion region is extremely high, thereby the CN has limited influence on the combustion process.

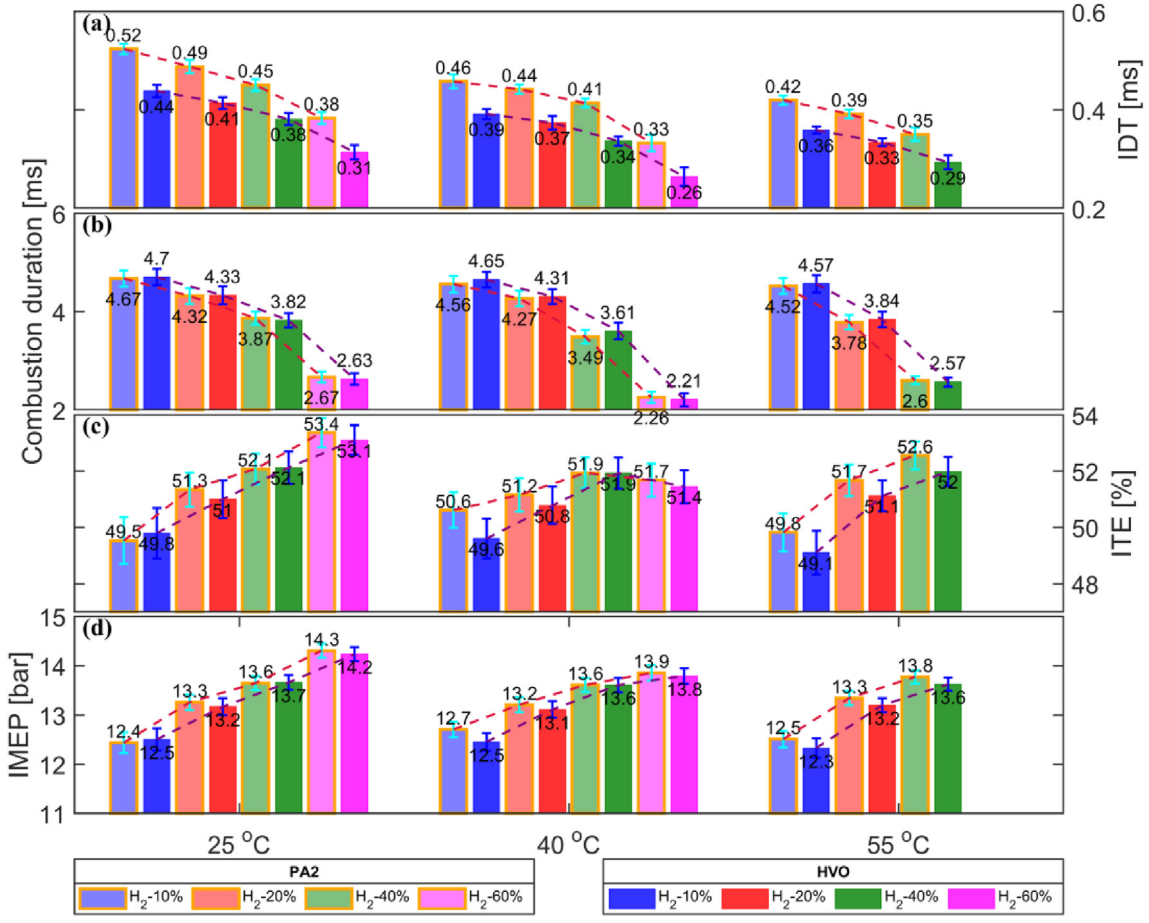

Fig. 6 – Effect of CN on engine performance at various M_{H2} and T_{air} conditions, (a) IDT, (b) combustion duration, (c) ITE, (d) IMEP.

According to the previous study, the CN plays a crucial role on engine performance. To clarify the effect of CN on the TF combustion engine, i.e., IDT (basedon PRR), combustion duration (based on CA90), ITE and IMEP are comprehensively compared and shown in Fig. 6. An evident difference in IDT (Fig. 6(a)) and combustion duration (Fig. 6(b)) can be observed in HVO and PA2. It is indicated that the higher CN fuel of HVO shows a shorter IDT but slightly longer combustion duration. The increase of the CN prolongs the combustion might be related to the shorter IDT, leading to less premixed pilot and H_2-CH_4-air followed by a slower burning rate during premixed combustion. However, the effect of CN on combustion duration is insignificant, maximum 0.12 ms (<1 CAD).

Fig. 6(c) and (d) present the effect of CN on IMEP and ITE. At low T_{air} conditions ($T_{air} = 25\ ^{\circ}C$), the IMEP and ITE of PA2 and HVO are comparable and are increased with the addition of H_2. It can be observed that the increase of IMEP is up to 1.9 bar and ITE is 3.8%. Nevertheless, increasing the M_{H2} shows a less effect or even a negative effect on ITE at moderate T_{air} conditions ($T_{air} = 25\ ^{\circ}C$) due to the abnormal combustion, such as knocking. Further increasing the T_{air} to 55 °C shows the same trends with the $T_{air} = 25\ ^{\circ}C$ conditions. It is indicated that the addition of H_2 shows a more significant effect on engine performance than the effect of charge-air temperature. Compared with T_{air}, the addition of the H_2 not only improves the reactivity of the charge mixture but also promotes the combustion process due to its excellent combustion properties. A comprehensive comparison of the effect of CN on IMEP and ITE indicates that the lower CN fuel PA2 exhibits a higher IMEP and ITE than HVO at all test conditions, especially at $T_{air} = 40\ ^{\circ}C$ and $M_{H2} = 10\%$, the maximum difference in ITE is ~1%. This most likely resulted from the higher CN of HVO, which leads to a shorter IDT, resulting in a less ignitable diesel cloud for ignition kernels formation during the premixed combustion stage. This drawback leads to a longer combustion duration after CA50 and lowers combustion efficiency. Moreover, the short IDT of high CN fuel may induce earlier end-gas autoignition and strong pressure oscillation, which could also reduce the ITE.

Effect of cetane number (CN) on combustion stability

Fig. 7 illustrates the effect of CN on combustion stability at various combustion states, such as normal combustion (Fig. 7 I), PREMIER combustion (Fig. 7 II) and knocking (Fig. 7 III). In each subplot, the top-right plot (a) presents the bandpass pressures. The top-right (b) and bottom-right (c) demonstrate the contour of resonant frequency and intensity at various

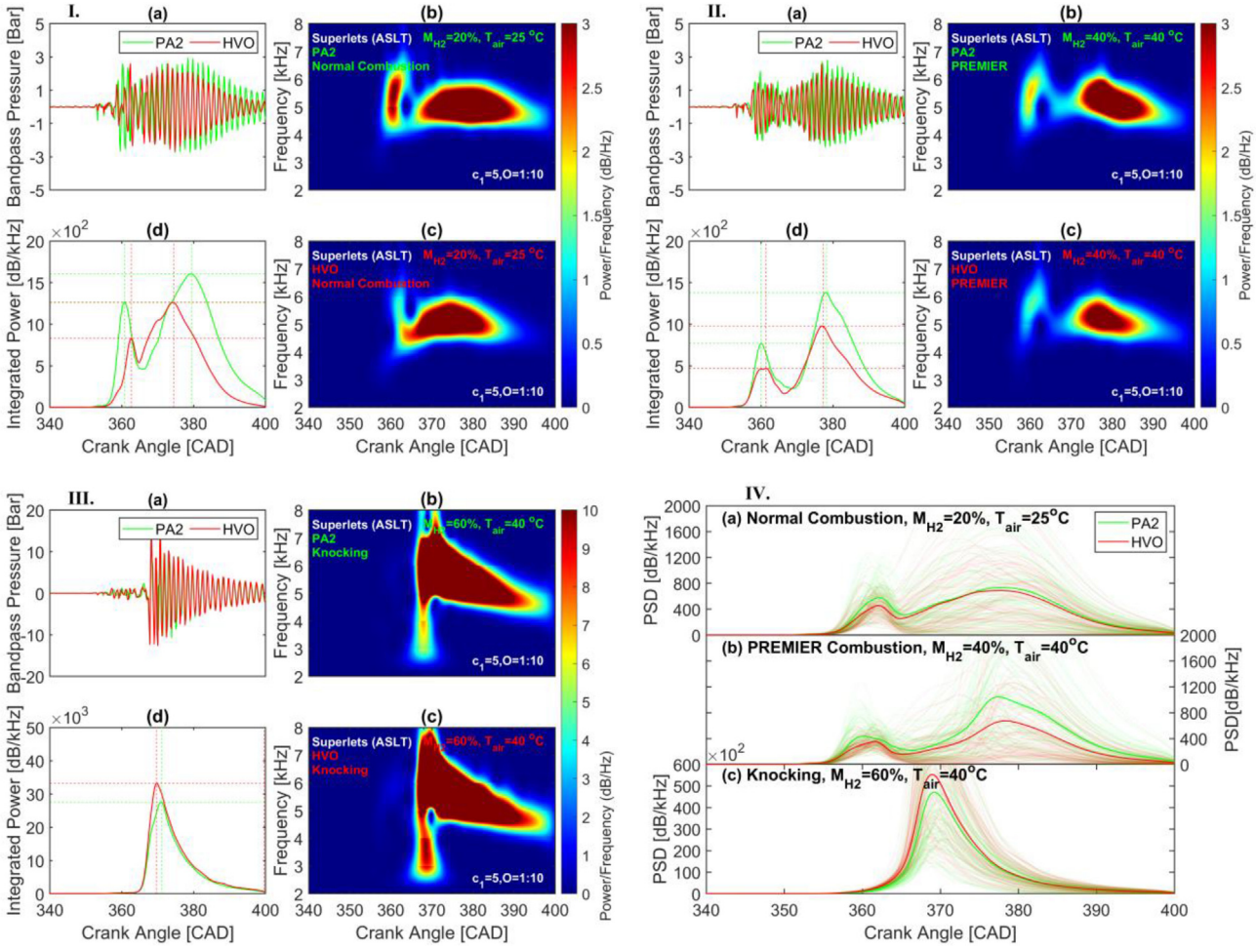

Fig. 7 – Effect of CN on combustion stability, I. normal combustion, II. PREMIER combustion, III. knocking, IV. integrated PSD comparison.

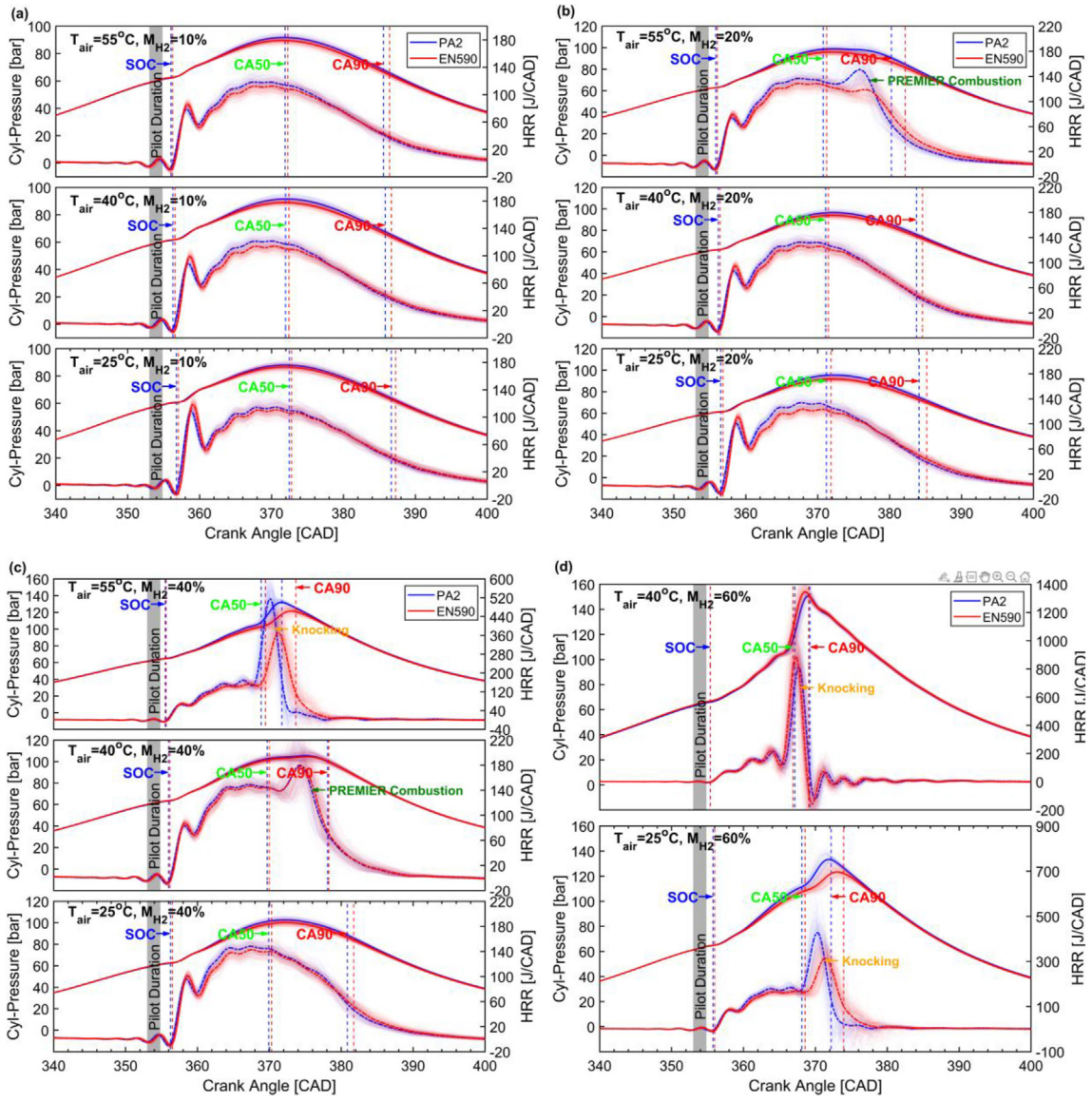

Fig. 8 – Effect of AC on in-cylinder pressure and aHRR at different M_{H2} and T_{air} conditions, (a) M_{H2} = 10%, (b) M_{H2} = 20%, (c) M_{H2} = 40%, (d) M_{H2} = 60%.

crank angles by the SL method. The bottom-right (d) presents power spectral density (PSD). Finally, the cyclic (transparent curves) and averaged (solid curves) are illustrated in Fig. 7 IV.

Fig. 7 I presents the time-frequency spectra of the in-cylinder pressure at HVO and PA2 of normal combustion conditions (M_{H2} = 20% and T_{air} = 25 °C). It can be observed that PA2 exhibits stronger pressure oscillation and longer oscillation duration than HVO in bandpass pressure. It can be attributed to the lower CN of PA2, resulting in a longer IDT and unstable ignition and premixed combustion process. At PREMIER combustion conditions, the dwell between the first-stage and second-stage combustion is enlarged, but the oscillation intensity of the first-stage combustion is lower. This is related to the shorter IDT at PREMIER combustion conditions as shown in Fig. 7 II, which leads to a less volume or cloud pocket in the pilot fuel and H_2-CH_4-air mixture subsequent to be weaker combustion during the premixed stage. PA2 shows a higher integrated power than HVO in both stages due to the longer IDT leads to more evident flame transition. In knocking mode (M_{H2} = 60% and T_{air} = 40 °C) as shown in Fig. 7 III, two-stage combustion is combined into single-stage combustion due to the high reactivity of charge mixture with the increase of the M_{H2} and T_{air}.

The integrated power of pressure oscillation (Fig. 7 IV) indicates that the resonant intensity peak of knocking is ~50 times stronger than normal and PREMIER combustion (based on peak PSD). However, in knocking mode, HVO presents a stronger resonant intensity than PA2. This most likely resulted from the higher CN of HVO advances the ignition timing and simultaneously promotes an earlier auto-ignition in the end-gas region and leads to a more violate combustion. Fig. 7 IV shows the cyclic and averaged integrated oscillation power. It is indicated that the CN has an insignificant effect on the combustion stability at low M_{H2} and T_{air} conditions (normal

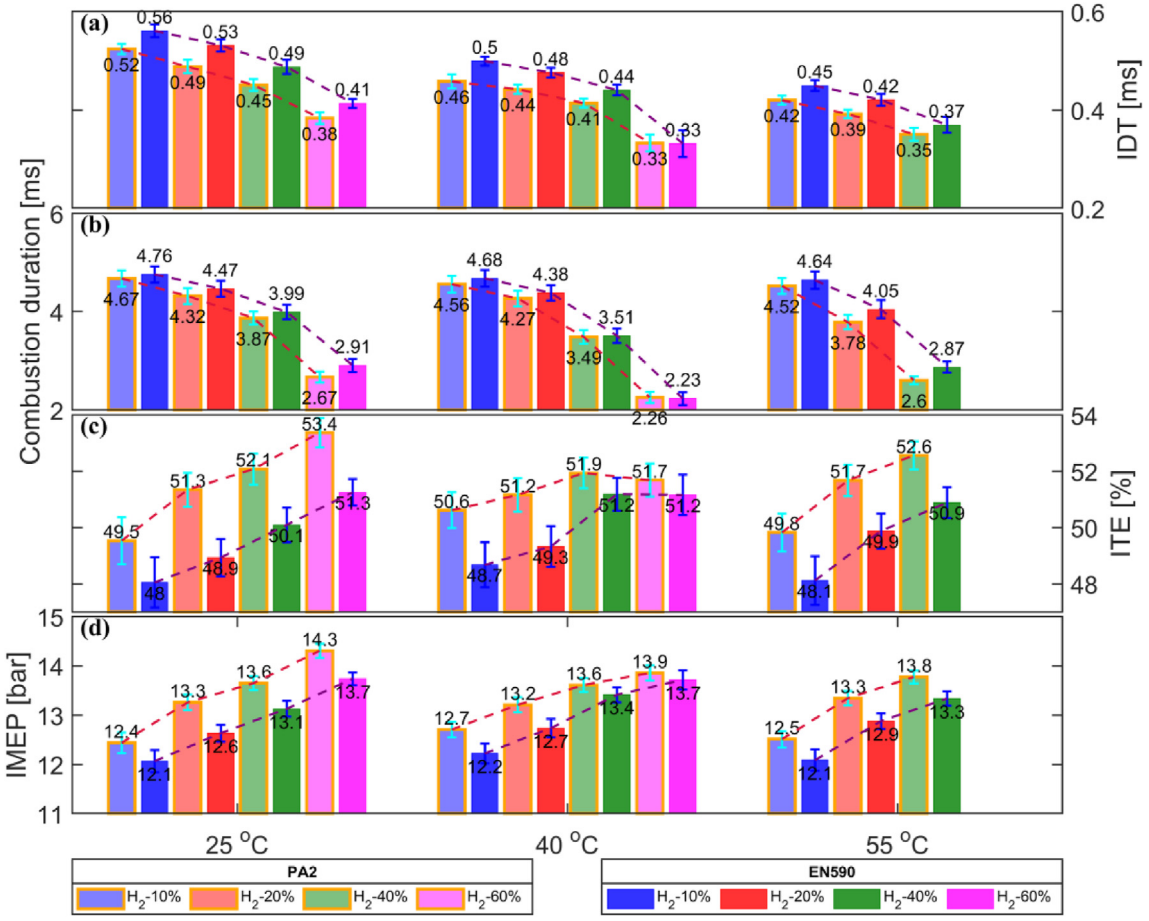

Fig. 9 – Effect of AC on engine performance at various M_{H2} and T_{air} conditions, (a) IDT, (b) combustion duration, (c) ITE, (d) IMEP.

combustion). With the increase of the M_{H2} or T_{air}, the difference of the integrated oscillation power is enlarged. The lower CN fuel exhibits stronger oscillation in PREMIER combustion but weaker oscillation in knocking. The interpretation is that in PREMIER combustion the relatively longer IDT of lower CN fuel has longer ignition and premixed combustion process, which leads to lower combustion stability. However, at knocking conditions, the higher CN fuel extremely shortens IDT and promotes the end-gas autoignition, thereby resulting in more violate combustion and stronger pressure oscillation.

The more comprehensive comparison of the effect of CN on combustion stability is summarized as the averaged in-cylinder pressure oscillation intensity, as shown in Appendix A1.

Effect of aromatic content (AC) on engine performance

In this section, a comprehensive comparison of the effect of AC on engine performance is investigated by comparing PA2 and EN590 at various T_{air} and/or M_{H2} conditions.

In general, high AC fuels have slower physical processes (e.g, evaporation and oxidation) and worse thermal decomposition compared to non-aromatic fuels (e.g. paraffin and naphthenes) due to the strong bonds connection in aromatic hydrocarbons [62]. The lower decomposition rate of not only the aromatic component but also other heavy saturated hydrocarbons will result in a higher concentration of low-boiling point hydrocarbons after the ignition compared to aromatic-free fuel [63].

To clarify the effect of AC on TF combustion, the PA2 and EN590 which have a similar CN value but different AC are selected for comparison. As shown in Table 5, PA2 is an aromatic-free fuel (AC<0.1) but EN590 has a high aromatic content (AC≈30). Fig. 8 depicts the effect of AC on cylinder pressure and HRR at a variety of M_{H2} and T_{air} conditions. From the aHRR profile, it can be observed that EN590 exhibits a longer IDT, resulting in stronger premixed combustion but a slower combustion rate during the main combustion at all conditions. Moreover, the combustion duration with lower AC is shorter than the higher AC fuel. The results indicate that besides the CN on the IDT and combustion duration, AC also plays an important role in IDT and combustion duration. The pilot fuel with lower AC can be decomposed and oxidized easily during ignition and premixed combustion process, which also promotes the combustion rate during the main combustion. Contrarily, the pilot fuel with higher AC has poor decomposition and oxidation behavior and thermal cracking due to the stronger carbon bond connection in aromatic rings, which prolongs the IDT and slowers the premixed and main combustion. Additionally, the appearance of the low-boiling point hydrocarbons generated by the aromatic components and other heavy saturated hydrocarbons after ignition may cause

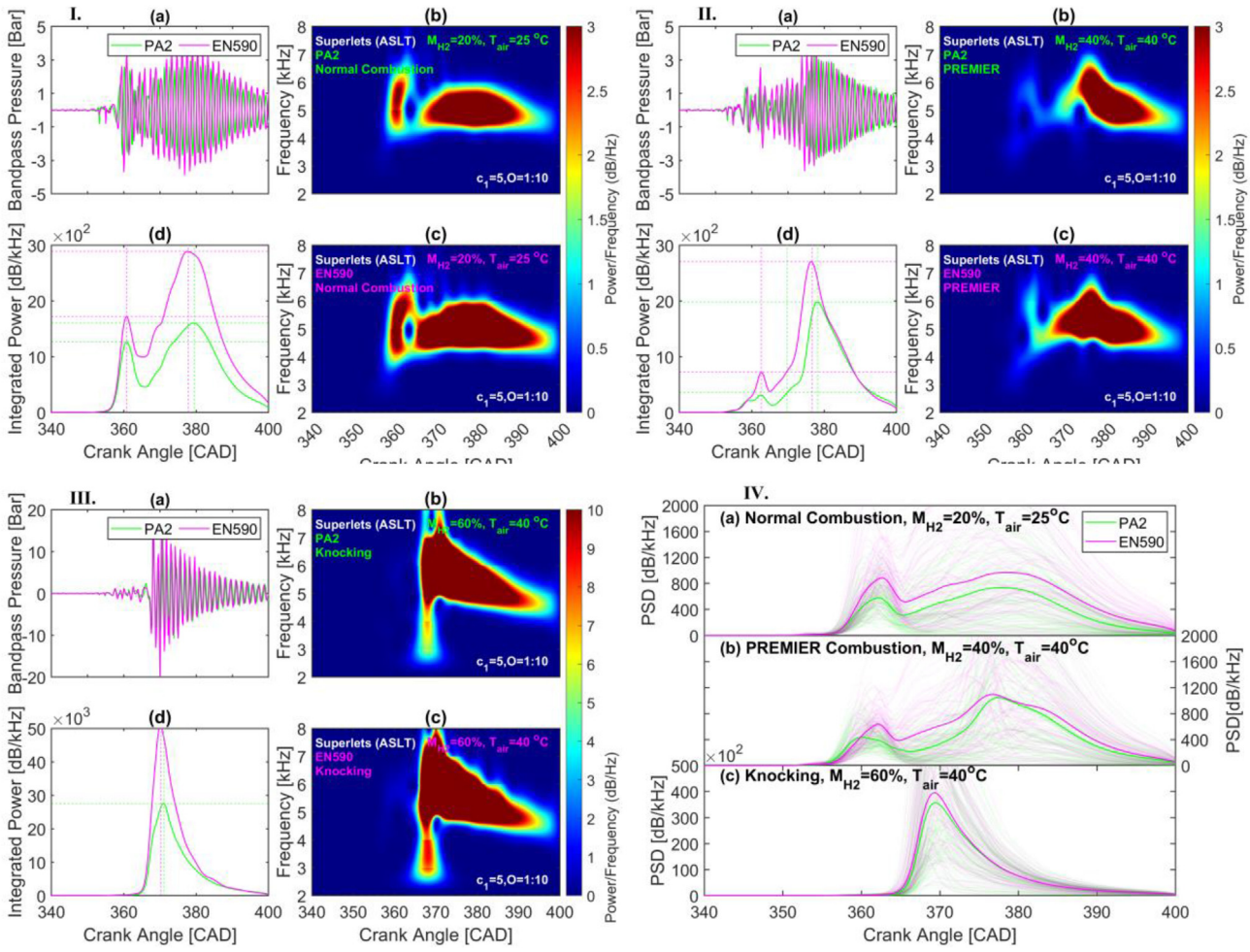

Fig. 10 – Effect of AC on combustion stability based on SL analysis at different combustion states, I. normal combustion, II. PREMIER combustion, III. knocking, IV. integrated PSD comparison.

incomplete combustion. However, at heavy-knocking conditions (M_{H2} = 60% and T_{air} = 40 °C), owing to the high H_2 concentration and high temperature in the cylinder (>950 K), the decomposition of the aromatic-containing fuel is promoted and most of the heavy hydrocarbon (C11 or above) components are cracked and oxidized completely [44]. Therefore, EN590 exhibits a slightly higher aHRR peak than PA2. Fig. 8

Fig. 9 (a) and (b) summarizes the effect of AC on the TF combustion engine, i.e., IDT (based on PRR), combustion duration (based on CA90). It is observed that the lower AC fuel PA2 shows a shorter IDT and combustion duration at most corresponding conditions. The explanation can be by considering the oxidation reaction pathway of aromatic hydrocarbons in diesel engines, which has been described in mechanistic studies in the literature [44–46,59,60,63,64], and can also be applied to the DF or TF combustion. According to the above studies, the higher AC fuel consumes more OH radicals in stabilizing benzyl radicals, reducing the pool of reactive radical species required for ignition and resulting in longer IDT [44]. Moreover, compared to the aromatic-free fuel, the aromatic-containing fuel is decomposed with difficulty because of the lower decomposition and oxidization rate of not only aromatic components but also other heavy saturate hydrocarbons, resulting in a higher concentration of low-boiling point hydrocarbons after the ignition [44]. Therefore, EN590 also shows a longer combustion duration compared with PA2.

Fig. 9 (c) and (d) depict the effect of AC on ITE at different M_{H2} and T_{air} conditions. It can be observed that the engine performance of TF combustion is highly dependent on the AC of pilot fuel. The lower AC fuel PA2 has higher IMEP and ITE compared with the higher AC fuel EN590. The maximum difference of IMEP and ITE occurs at M_{H2} = 20% and T_{air} = 25 °C, which is up to0.7 bar and 2.4%, respectively. The results indicate that lower AC fuel is easy to be decomposed and oxidized, which promotes the ignition and combustion process, resulting in a better fuel energy conversion efficiency. On contrary, a lower IMEP and ITE observed for high AC pilot fuel combustion is related to the poor thermal decomposition and oxidization process of aromatic hydrocarbons, which produces a high-temperature region locally and leads to slow and incomplete combustion [42,44].

The more comprehensive comparison of the effect of AC on combustion stability is summarized as the averaged in-cylinder pressure oscillation intensity, as shown in Appendix A2.

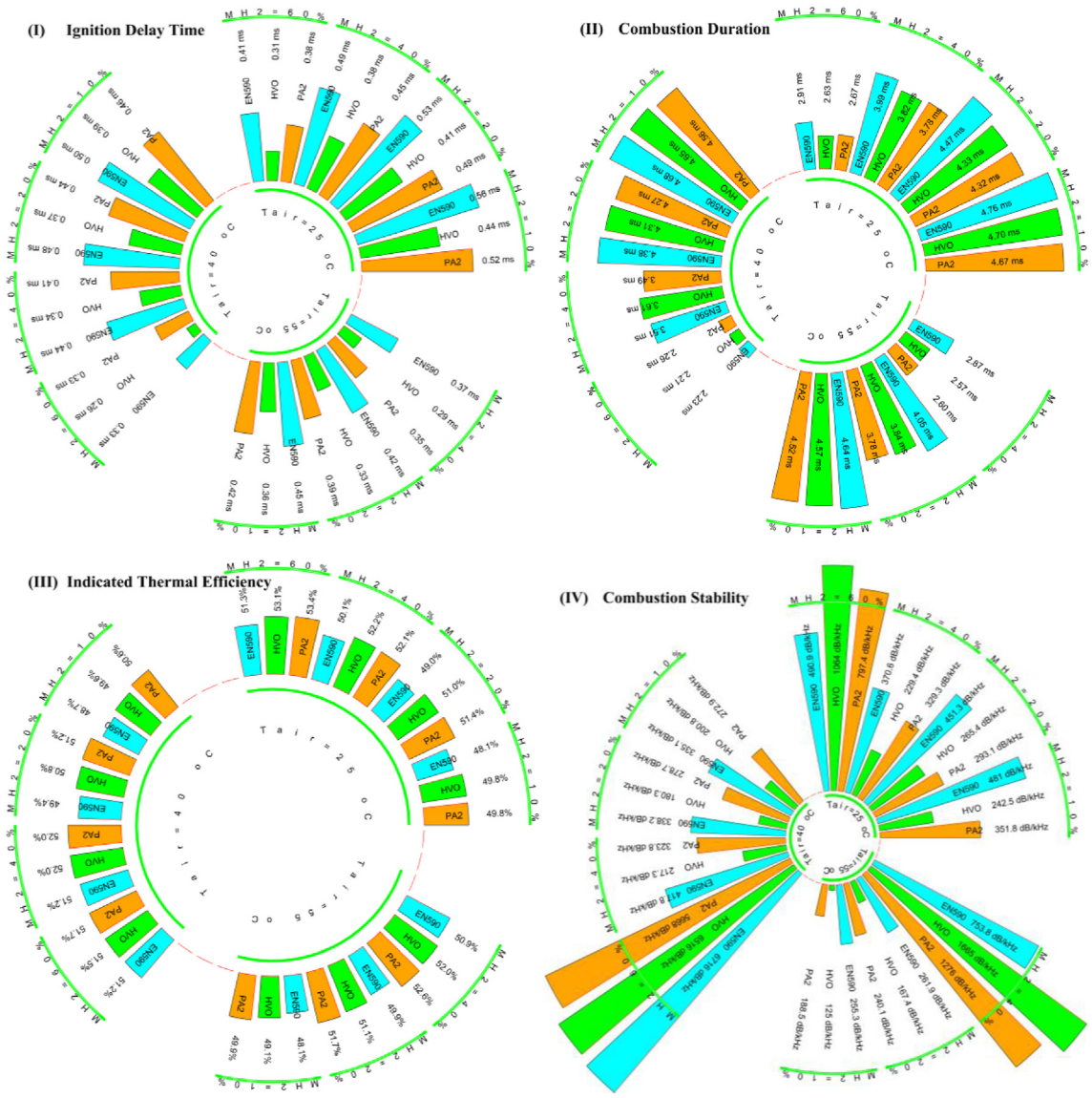

Fig. 11 – Comprehensive comparison of the pilot fuel properties on the TF combustion at various charge-air temperature and H2 concentration conditions. (I) Ignition delay time, (II) combustion duration, (III) indicated thermal efficiency, (IV) combustion stability.

Effect of aromatic content (AC) on combustion stability

Fig. 10 summarizes the effect of AC on combustion stability at various combustion states, such as normal combustion (Fig. 10 I), PREMIER combustion (Fig. 10 II) and knocking (Fig. 10 III), and the integrated PSD comparison of the PA2 and EN590 in different combustion states is shown in Fig. 10 IV.

Fig. 11 I shows that two-stage combustion can be observed in both PA2 and EN590, as explained in Effect of cetane number (CN) on combustion stability. The EN590 shows higher integrated power of pressure oscillation than PA2 in both premixed and main combustion stages. This is because the poor decomposition and oxidation behavior of the aromatic hydrocarbons prolonged the ignition and premixed combustion process, which generates more pressure oscillation during the premixed combustion stage. In the main combustion stage, the longer IDT of EN590 creates larger premixed flame clouds and induces more pressure oscillation due to the flame transition. At PREMIER combustion conditions, Fig. 10 II indicates that the integrated power at the premixed combustion stage is lower than that of the main combustion stage, also than that of the normal combustion. This is related to the more reactive environment at PREMIER combustion conditions, the shorter IDT reduced the premixing time between pilot fuel and charge mixtures. Thereby, after a short and weak premixed combustion, the combustion directly shifts to the main combustion. Again, the integrated power of pressure oscillation of EN590 is larger than PA2. The poor combustion stability at normal and PREMIER combustion conditions indicates that the poor decomposition and oxidization behavior of high AC fuel could reduce the combustion stability in TF combustion. As explained in 4.3, the high AC

pilot fuel in the mixture acts as a sink to remove OH radicals during the ignition delay period, preventing the build-up of sufficient radicals to initiate ignition throughout the cylinder charge. Thus, a longer time is needed to create a stable flame kernel during the first stage, and additional time is required for more fuel and air to mix to near-stoichiometric conditions for combustion in the second stage. Additionally, the pilot fuel with high AC can produce a high-temperature region locally because the hydrocarbons with ring structures tend to have higher adiabatic flame temperatures [58], which physically reduces the combustion stability due to the inhomogeneity of the high-temperature distribution in the cylinder. Moreover, on the point of the chemical process, fuels with aromatics are cracked with difficulty [12], resulting in more unstable flame propagation in the cylinder.

Fig. 10 IV shows the cyclic and averaged integrated oscillation power. It is indicated that the AC has a significant effect on the combustion stability at low M_{H2} and T_{air} conditions (normal combustion). With the increase of the M_{H2} or T_{air}, the difference in the integrated oscillation power is reduced. The interpretation is that the increase of the M_{H2} or T_{air} improves the reactivity of the charge mixture enhanced the decomposition and oxidization process of aromatic hydrocarbons.

Summary of the results

Fig. 11 summarizes the outcome of this work based on the engine performance and combustion stability analysis, results and averaged trends observed for all three pilot fuels. A comprehensive comparison for IDT, combustion duration, ITE and combustion stability can be seen in Fig. 11. In summary, it is found out that 1) the CN of the pilot fuel is the most important factor which influences the autoignition process, a fuel with higher CN exhibits a shorter IDT, while AC also affects the decomposition and oxidization process during the ignition period. In general, a low AC fuel shows a shorter IDT with a comparable CN. 2) Combustion duration is sensitive to the CN and AC due to their effects on the ignition and oxidization process during ignition and premixed combustion. The low AC and averaged CN pilot fuel shows the shortest combustion duration than others. 3) Owing to the effect of CN and AC on ignition and combustion characteristics, they have a significant impact on ITE. The pilot fuel with low AC can improve the ITE up to ~2.1% compared with high AC fuel (e.g., EN590). 4) CN and AC exhibit a dramatic effect on combustion stability. It is suggested that the pilot fuel with high CN has better combustion stability in normal and PREMIER combustion, but worse combustion stability in knocking combustion.

Conclusions

The effect of pilot fuel properties, especially the effect of CN and AC on the engine performance and combustion stability of TF combustion engine is experimentally studied in this paper. Three pilot fuels, a low aromatic fuel (PA2), renewable fuel (HVO), and European standard diesel (EN590) are comprehensively investigated at various M_{H2} and T_{air} conditions. The major findings from this study are summarized as follow:

(1) the IDT is predominantly determined by the CN of pilot fuel. A pilot fuel with higher CN shortens the IDT. Nevertheless, the presence of AC in pilot fuel prolongs the IDT due to its difficulty in thermal decomposition and oxidization at low in-cylinder temperatures.
(2) owing to the effect of the pilot fuel properties on the ignition and premixed combustion process, the CN and AC can influence the combustion duration as well. A pilot fuel with higher CN or/and lower AC has earlier ignition timing and weaker premixed combustion because of the limited mixing time between pilot fuel and CH_4-H_2-air mixture. This creates a smaller flame volume during premixed combustion and subsequent a relatively slower burning rate during the main combustion.
(3) CN and AC of pilot fuel exhibit a significant effect on the IMEP and ITE of TF combustion. A pilot fuel with low AC improves the IMEP up to 0.6 bar, corresponding to ~2.1% improvement in ITE. However, CN shows a margin effect on the IMEP and ITE.
(4) a significant effect of pilot fuel properties on combustion stability of TF combustion is observed in this study. It is indicated that a pilot fuel with higher CN or/and lower AC (e.g., PA2 and HVO) can improve the combustion stability at low or/and moderate M_{H2} and T_{air} conditions (normal and PREMIER combustion). However, at high M_{H2} or/and T_{air} conditions (knocking), higher CN and lower AC of the pilot fuel induces earlier autoignition in the end-gas region, which produces a stronger pressure oscillation.
(5) *Superlets* perform well on combustion stability investigation based on in-cylinder pressure, resolving high temporal and frequency resolution with excellent precision.

In summary, pilot fuel as an ignitor in DF or TF combustion plays a crucial role in engine performance and combustion stability. A pilot fuel with low aromatic content is always favorable for TF combustion because it can avoid difficulties in decomposition and oxidization during the ignition and premixed combustion process. Additionally, it can improve combustion efficiency and stability. A pilot fuel with high CN can shorten the IDT. However, this will also induce earlier end-gas autoignition, which may course knocking.

Declaration of competing interest

The authors declare that they have no known competing financial interests or personal relationships that could have appeared to influence the work reported in this paper.

Acknowledgments

The present study has been financially supported by the Academy of Finland (Grant Nos. 297248 and 318024). The authors are thankful to Ranta Olli and Blomstedt Otto for their supports on the engine preparations. The second author has

also received a scholarship from Fortum-Neste Foundation and Merenkulunsäätio under application no. 2020050 and 20210073, respectively.

Appendix A. Supplementary data

The following is the supplementary data to this article:

Appendix 1. Effect of the PA2 and HVO on the averaged pressure oscillation intensity

Fig. A1 presents the effect of PA2 and HVO on combustion stability at corresponding conditions. The combustion stability is assessed based on the averaged pressure oscillation intensity. The results indicate that higher CN fuel improves combustion stability, especially at lower M_{H2} and T_{air} conditions (e.g., normal and PREMIER combustion). However, when the addition of the M_{H2} or the increase of the T_{air} is exceeding a specific value, the occurrence of knocking shows an opposite trend. It is observed that the fuel with a higher CN exhibits stronger pressure oscillation intensity and lower combustion stability due to the earlier ignition time induces the earlier end-gas autoignition.

Appendix 2. Effect of the PA2 and EN590 on the averaged pressure oscillation intensity

Fig. A2 summarizes the effect of AC on combustion stability in TF combustion based on the averaged pressure oscillation intensity. It is shown that the pilot fuel with lower AC (e.g., PA2) shows better combustion stability than higher AC fuel (e.g., EN590) in most of the corresponding conditions. The explanation is that, in normal or PREMIER combustion modes, the higher AC decreases the combustion stability by the difficulty in thermal decompositions of aromatic hydrocarbons and slow physical process, which in turn leads to locally fuel-rich regions [14]. However, in heavy-knocking mode (M_{H2} = 60% and T_{air} = 40 °C), PA2 exhibits worse combustion stability than EN590. This is related to the better decomposition and oxidization of aromatic-free fuel PA2, which leads to a shorter IDT and induces earlier end-gas autoignition at this high reactivity conditions and consequent to earlier spontaneous combustion in the main and end-gas regions and stronger pressure fluctuation. Contrarily, the poor decomposition property of high AC EN590 prolongs the ignition process and slows down the spontaneous combustion in the main and end-gas regions, resulting in a less violate combustion.

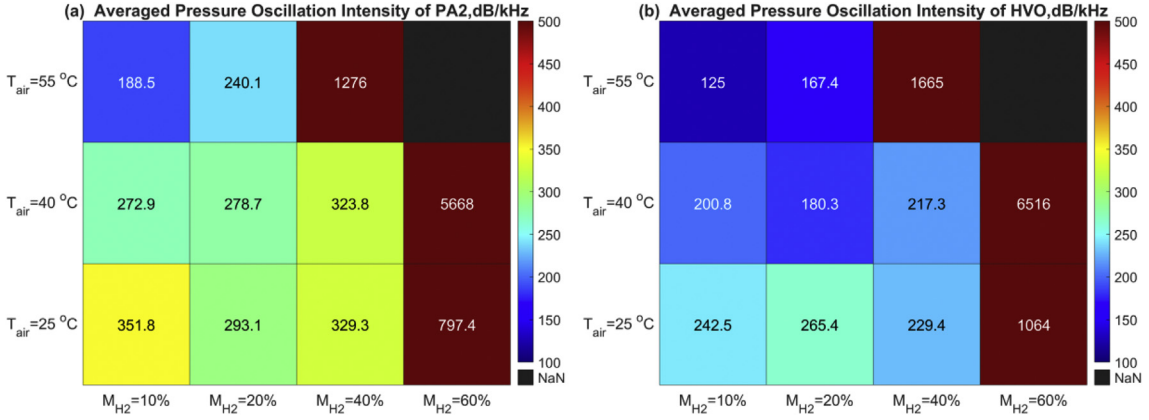

Fig. A1 – Averaged pressure oscillation intensity of (a) PA2, (b) HVO at different M_{H2} and T_{air} conditions.

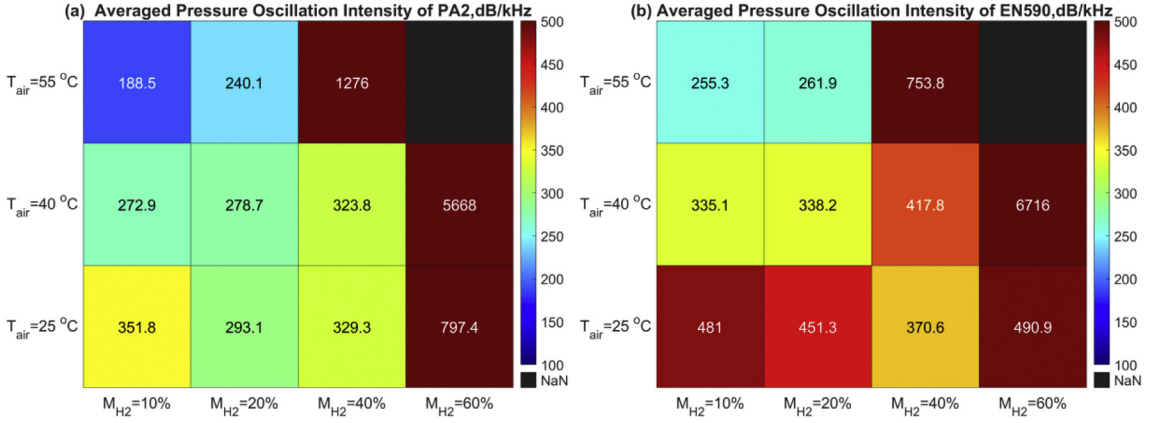

Fig. A2 – Averaged pressure oscillation intensity of (a) PA2, (b) EN590 at different M_{H2} and T_{air} conditions.

REFERENCES

[1] European Parliament. CO2 emissions from cars: facts and figures (Infographics). 2021. Retrieved 05 02, 2021, from Europarl, https://www.europarl.europa.eu/news/en/headlines/society/20190313STO31218/co2-emissions-from-cars-facts-and-figures-infographics.

[2] Tutak Wojciech, Jamrozik Arkadiusz, Grab-Rogaliński Karol. Effect of natural gas enrichment with hydrogen on combustion process and emission characteristic of a dual fuel diesel engine. Int J Hydrogen Energy 2020;45(15):9088–97.

[3] Lee Chia-fon, Pang Yuxin, Wu Han, Hernández Juan J, Zhang Saifei, Liu Fushui. The optical investigation of hydrogen enrichment effects on combustion and soot emission characteristics of CNG/diesel dual-fuel engine. Fuel 2020;280. 118639.

[4] Jin Kusaka, Okamoto Takashi, Daisho Yasuhiro, Kihara Ryouji, Saito Takeshi. Combustion and exhaust gas emission characteristics of a diesel engine dual- fueled with natural gas. JSAE Rev 2000;21(4):489–96.

[5] Rosha Pali, Amit Dhir, Mohapatra Saroj Kumar. Influence of gaseous fuel induction on the various engine characteristics of a dual fuel compression ignition engine: a review. Renew Sustain Energy Rev 2018;82(Part 3):3333–49.

[6] Verhelst Sebastian, Wallner Thomas. Hydrogen-fueled internal combustion engines. Prog Energy Combust Sci 2009;35(6):490–527.

[7] Hegab Abdelrahman, La Rocca Antonino, Paul Shayler. Towards keeping diesel fuel supply and demand in balance: dual-fuelling of diesel engines with natural gas. Renew Sustain Energy Rev 2017;70:666–97.

[8] Sahoo BB, Sahoo N, Saha UK. Effect of engine parameters and type of gaseous fuel on the performance of dual-fuel gas diesel engines – a critical review. Renew Sustain Energy Rev 2009;13:1151–84.

[9] Paul A, Bose PK, Panua RS, Banerjee R. An experimental investigation of performance-emission trade off of a CI engine fueled by diesel–compressed natural gas (CNG) combination and diesel–ethanol blends with CNG enrichment. Energy 2013;55:787–802.

[10] Lounici MS, Loubar K, Tarabet L, Balistrou M, Niculescu D, Tazerout M. Towards improvement of natural gas–diesel dual fuel mode: an experimental investigation on performance and exhaust emissions. Energy 2014;64:2000–11.

[11] Cheenkachorn K, Poompipatpong C, Ho CG. Performance and emissions of a heavy-duty diesel engine fuelled with diesel and LNG (liquid natural gas). Energy 2013;53:52–7.

[12] Ryu K. Effects of pilot injection timing on the combustion and emissions characteristics in a diesel engine using biodiesel–CNG dual fuel. Appl Energy 2013;111:721–30.

[13] Mehra Roopesh Kumar, Duan Hao, Juknelevičius Romualdas, Ma Fanhua, Li Junyin. Progress in hydrogen enriched compressed natural gas (HCNG) internal combustion engines - a comprehensive review. Renew Sustain Energy Rev 2017;80:1458–98.

[14] Deb Madhujit, Paul Abhishek, Debroy Durbadal, et al. An experimental investigation of performance-emission trade off characteristics of a CI engine using hydrogen as dual fuel. Energy 2015;85:569–85.

[15] Szwaja S, Naber JD. Dual nature of hydrogen combustion knock. Int J Hydrogen Energy 2013;38(28):12489–96.

[16] Luo QH, Sun BG. Inducing factors and frequency of combustion knock in hydrogen internal combustion engines. Int J Hydrogen Energy 2016;41(36):16296–305.

[17] Verhelst S, Wallner T. Hydrogen-fueled internal combustion engines. Prog Energy Combust Sci 2009;35(6):490–527.

[18] Duan J, Liu F, Sun B. Backfire control and power enhancement of a hydrogen internal combustion engine. Int J Hydrogen Energy 2014;39(9):4581–9.

[19] Said Lounici Mohand, Boussadi Asma, Loubar Khaled, Tazerout Mohand. Experimental investigation on NG dual fuel engine improvement by hydrogen enrichment. Int J Hydrogen Energy 2014;39(36):21297–306.

[20] Zheng J, Hu E, Huang Z, Ning D, Wang J. Combustion and emission characteristics of a spray guided direct-injection spark-ignition engine fueled with natural gas–hydrogen blends. Int J Hydrogen Energy 2011;36:11155–63.

[21] Zhou JH, Cheung CS, Leung CW. Combustion, performance and emissions of a diesel engine with H2, CH4 and H2–CH4 addition. Int J Hydrogen Energy 2014;39(9):4611–21.

[22] Mansor MRA, Abbood MM, Mohamad TI. The influence of varying hydrogen-methane-diesel mixture ratio on the combustion characteristics and emissions of a direct injection diesel engine. Fuel 2017;190:281–91.

[23] Cheng Qiang, Ahmad Zeeshan, Kaario Ossi, Vuorinen Ville, Larmi Martti. Experimental study on tri-fuel combustion using premixed methane-hydrogen mixtures ignited by a diesel pilot. Int J Hydrogen Energy 2021;46(40):21182–97.

[24] Said Lounici Mohand, Boussadi Asma, Loubar Khaled, Tazerout Mohand. Experimental investigation on NG dual fuel engine improvement by hydrogen enrichment. Int J Hydrogen Energy 2014;39(36):21297–306.

[25] Liew C, Li H, Nuszkowski J, Liu S, Gatts T, Atkinson R, et al. An experimental investigation of the combustion process of a heavy-duty diesel engine enriched with H2. Int J Hydrogen Energy 2010;35:11357–65.

[26] Xie Yongliang, Sun ZY. Effects of the external turbulence on centrally-ignited spherical unstable Ch4/H2/air flames in the constant-volume combustion bomb. Int J Hydrogen Energy 2019;44(36):20452–61.

[27] Stewart J, Clarke A, Chen R. An experimental study of the dual-fuel performance of a small compression ignition diesel engine operating with three gaseous fuels. Proc Inst Mech Eng J Automot Eng 2007;221(D8):943–56.

[28] Park C, Kim C, Choi Y, Won S, Moriyoshi Y. The influences of hydrogen on the performance and emission characteristics of a heavy duty natural gas engine. Int J Hydrogen Energy 2011;36:3739–45.

[29] Karagoz Y, Guler I, Sandalci T, Yuksek L, Dalkilic AS, Wongwises S. Effects of hydrogen and methane addition on combustion characteristics, emissions, and performance of a CI engine. Int J Hydrogen Energy 2016;41:1313–25.

[30] Abu-Jrai Ahmad M, Al-Muhtaseb Ala'a H, Hasan Ahmad O. Combustion, performance, and selective catalytic reduction of NOx for a diesel engine operated with combined tri fuel (H2, CH4, and conventional diesel). Energy 2017;119:901–10.

[31] Sandalcı Tarkan, Işın Övün, Galata Serkan, Karagöz Yasin, Güler İlker. Effect of hythane enrichment on performance, emission and combustion characteristics of an ci engine. Int J Hydrogen Energy 2019;44(5):3208–20.

[32] Abu-Jrai AM, Al-Muhtaseb AH, Hasan AO. Combustion, performance, and selective catalytic reduction of NOx for a diesel engine operated with combined tri fuel (H2, CH4, and conventional diesel). Energy 2017;119:901–10.

[33] McTaggart-Cowan CP, Rogak SN, Munshi SR, Hill PG, Bushe WK. Combustion in a heavy-duty direct-injection engine using hydrogen-methane blend fuels. Int J Engine Res 2009;10(1):1–13.

[34] Karimkashi Shervin, Kahila Heikki, Kaario Ossi, Larmi Martti, Vuorinen Ville. Numerical study on tri-fuel combustion: ignition properties of hydrogen-enriched methane-diesel and methanol-diesel mixtures. Int J Hydrogen Energy 2020;45(7):4946–62.

[35] Tüchler Stefan, Dimitriou Pavlos. On the capabilities and limitations of predictive, multi-zone combustion models for hydrogen-diesel dual fuel operation. Int J Hydrogen Energy 2019;44(33):18517–31.
[36] Karimkashi Shervin, Kahila Heikki, Kaario Ossi, Larmi Martti, Vuorinen Ville. A numerical study on combustion mode characterization for locally stratified dual-fuel mixtures. Combust Flame 2020;214:121–35.
[37] Liu Jinlong, Dumitrescu Cosmin E. Single and double Wiebe function combustion model for a heavy-duty diesel engine retrofitted to natural-gas spark-ignition. Appl Energy 2019;248:95–103.
[38] Alrazen HA, Abu Talib A, Ahmad K. A two-component CFD studies of the effects of H2, CNG, and diesel blend on combustion characteristics and emissions of a diesel engine. Int J Hydrogen Energy 2016;41:10483–95.
[39] Mansor MRA, Abbood MM, Mohamad TI. The influence of varying hydrogen-methane-diesel mixture ratio on the combustion characteristics and emissions of a direct injection diesel engine. Fuel 2017;190:281–91.
[40] Ebrahimi Mojtaba, Jazayeri Seyed Ali. Effect of hydrogen addition on RCCI combustion of a heavy duty diesel engine fueled with landfill gas and diesel oil. Int J Hydrogen Energy 2019;44(14):7607–15.
[41] Liu J, Yang F, Wang H, Ouyang M. Numerical study of hydrogen addition to DME/CH4 dual fuel RCCI engine. Int J Hydrogen Energy 2012;37:8688–97.
[42] McTaggart-Cowan CP, Rogak SN, Munshi SR, Hill PG, Bushe WK. Combustion in a heavy-duty direct-injection engine using hydrogen-methane blend fuels. Int J Engine Res 2009;10(1):1–13.
[43] Bose PK, Maji D. An experimental investigation on engine performance and emissions of a single cylinder diesel engine using hydrogen as inducted fuel and diesel as injected fuel with exhaust gas recirculation. Int J Hydrogen Energy 2009;34(11):4847–54.
[44] Ahmad Zeeshan, Kaario Ossi, Cheng Qiang, Larmi Martti. Effect of pilot fuel properties on lean dual-fuel combustion and emission characteristics in a heavy-duty engine. Appl Energy 2021;282(Part A):116134. https://doi.org/10.1016/j.apenergy.2020.116134.
[45] Kee S, Mohammadi A, Kidoguchi Y, Miwa K. Effects of aromatic hydrocarbons on fuel decomposition and oxidation processes in diesel combustion. SAE Technical Paper 2005-01-2086; 2005. https://doi.org/10.4271/2005-01-2086.
[46] Jeihouni Y, Pischinger S, Ruhkamp L, Koerfer T. Relationship between fuel properties and sensitivity analysis of non-aromatic and aromatic fuels used in a single cylinder heavy duty diesel engine. SAE Technical Paper 2011-01-0333; 2011. https://doi.org/10.4271/2011-01-0333.
[47] García Antonio, Monsalve-Serrano Javier, Villalta David, Lago Sari Rafael, Gordillo Zavaleta Victor, Gaillard Patrick. Potential of e-Fischer Tropsch diesel and oxymethyl-ether (OMEx) as fuels for the dual-mode dual-fuel. concept. Appl Energy 2019;253:113622.
[48] Imran S, Korakianitis T, Shaukat R, Farooq M, Condoor S, Jayaram S. Experimentally tested performance and emissions advantages of using natural-gas and hydrogen fuel mixture with diesel and rapeseed methyl ester as pilot fuels. Appl Energy 2018;229:1260–8.
[49] Tarabet L, Lounici MS, Loubar K, Khiari K, Bouguessa R, Tazerout M. Hydrogen supplemented natural gas effect on a DI diesel engine operating under dual fuel mode with a biodiesel pilot fuel. Int J Hydrogen Energy 2018;43(11):5961–71.
[50] Gadalla Mahmoud, Kannan Jeevananthan, Bulut Tekgül, Karimkashi Shervin, Kaario Ossi, Vuorinen Ville. Large-eddy simulation of tri-fuel combustion: diesel spray assisted ignition of methanol-hydrogen blends. Int J Hydrogen Energy 2021;46(41):21687–703.
[51] Oliva Fermín, Fernández-Rodríguez David. Autoignition study of LPG blends with diesel and HVO in a constant-volume combustion chamber. Fuel 2020;267:117173.
[52] Cheng Qiang, Tuomo Hulkkonen, Kaario Ossi, Martti Larmi. Spray dynamics of HVO and EN590 diesel fuels. Fuel 2019;245:198–211.
[53] Deb Madhujit, Paul Abhishek, Debroy Durbadal, Sastry GRK, Panua Raj Sekhar, Bose PK. An experimental investigation of performance-emission trade off characteristics of a CI engine using hydrogen as dual fuel. Energy 2015;85:569–85.
[54] Heywood JB. Internal combustion engine fundamentals. New York: McGraw-Hill, Inc; 1988.
[55] Lakshminarayanan PA, Aghav YV. Ignition delay in a diesel engine. In: Modelling diesel combustion. Mechanical engineering series. Dordrecht: Springer; 2010. https://doi.org/10.1007/978-90-481-3885-2_5.
[56] Kawahara Nobuyuki, Tomita Eiji. Visualization of auto-ignition and pressure wave during knocking in a hydrogen spark-ignition engine. Int J Hydrogen Energy 2009;34(7):3156–63.
[57] Kawahara Nobuyuki, Kim Yungjin, Wadahama Hisashi, Tsuboi Kazuya, Tomita Eiji. Differences between PREMIER combustion in a natural gas spark-ignition engine and knocking with pressure oscillations. Proc Combust Inst 2019;37(4):4983–91.
[58] Moca VV, Bârzan H, Nagy-Dăbâcan A, et al. Time-frequency super-resolution with superlets. Nat Commun 2021;12:337. https://doi.org/10.1038/s41467-020-20539-9.
[59] Han Manbae. The effects of synthetically designed diesel fuel properties – cetane number, aromatic content, distillation temperature, on low-temperature diesel combustion. Fuel 2013;109:512–9.
[60] Qian Yong, Qiu Yue, Zhang Yahui, Lu Xingcai. Effects of different aromatics blended with diesel on combustion and emission characteristics with a common rail diesel engine. Appl Therm Eng 2017;125:1530–8.
[61] Hellier P, Talibi M, Eveleigh A, Ladommatos N. An overview of the effects of fuel molecular structure on the combustion and emissions characteristics of compression ignition engines. Proc Inst Mech Eng - Part D J Automob Eng 2018;232(1):90–105.
[62] Naik C, Puduppakkam K, Meeks E. Impact of aromatics on engine performance. SAE Technical Paper 2019-01-0948; 2019. https://doi.org/10.4271/2019-01-0948.
[63] Zannis T, Hountalas D, Papagiannakis R, Levendis Y. Effect of fuel chemical structure and properties on diesel engine performance and pollutant emissions: review of the results of four European research programs. SAE Int. J. Fuels Lubr. 2009;1(1):384–419. https://doi.org/10.4271/2008-01-0838.
[64] Sienicki E, Jass R, Slodowske W, McCarthy C, et al. Diesel fuel aromatic and cetane number effects on combustion and emissions from a prototype 1991 diesel engine. SAE Technical Paper 902172; 1990. https://doi.org/10.4271/902172.